



1 Manuscript title:  
2 **A comparison of bacterial communities from OMZ sediments in the Arabian Sea and the Bay of Bengal**  
3 **reveals major differences in nitrogen turnover and carbon recycling potential**  
4

5 Author names:  
6 **<sup>1,2</sup>Jovitha Lincy \* and <sup>1</sup>Cathrine Sumathi Manohar**  
7

8 Author affiliation(s):  
9 **<sup>1</sup>Biological Oceanography Division, CSIR-National Institute of Oceanography (NIO), Goa-403004, India.**  
10 **<sup>2</sup>Academy of Scientific and Innovative Research (AcSIR), CSIR-NIO Campus, Goa, India.**  
11

12 Correspondence:  
13 **JL:** [jovithalincy@gmail.com](mailto:jovithalincy@gmail.com); +91-9847871900 (\* corresponding author).  
14 **CSM:** [cathrine@nio.org](mailto:cathrine@nio.org); +91-832-245-0441.  
15  
16  
17  
18  
19  
20  
21  
22  
23  
24  
25  
26  
27  
28  
29  
30



# 31 **ABSTRACT:**

32           The Northern Indian Ocean hosts two Oxygen Minimum Zones (OMZ), one in the Arabian Sea and the  
 33 other in the Bay of Bengal. High-throughput sequencing was used to understand the total bacterial diversity in,  
 34 the surface sediment off Goa within the OMZ of the Arabian Sea, and from off Paradip within the OMZ of the  
 35 Bay of Bengal. The dominant phyla identified included Firmicutes (33.08%) and Proteobacteria (32.59%) from  
 36 the Arabian Sea, and Proteobacteria (52.65%) and Planctomycetes (9.36%) from the Bay of Bengal. Only 30%  
 37 of OTUs were shared between the sites which make up three-fourth of the Bay of Bengal OMZ bacterial  
 38 community, but only one-fourth of the Arabian Sea OMZ sediment bacterial community. Statistical analysis  
 39 indicated the bacterial diversity from sediments of the Bay of Bengal OMZ is ~48% higher than the Arabian Sea  
 40 OMZ. The community analysis combined with a predictive functional profiling of 16S rRNA amplicons  
 41 pinpointed the occurrence of specific enzymes that are crucial in the cycling of nitrogen and sulfur compounds,  
 42 with major differences regarding nitrogen fixation and carbon recycling.

# 44 **Keywords:**

45 OMZ, sediment bacteria, 454 pyrosequencing, Arabian Sea, Bay of Bengal, functional ecology.

# 48 **1. INTRODUCTION**

49           The Northern Indian Ocean consists of two major ocean basins: the Arabian Sea (AS) in the west and  
 50 the Bay of Bengal (BoB) in the east. Even though both these basins are placed in the same latitude, they differ in  
 51 many aspects. This includes differences in average salinity, primary productivity, nitrogen loss, the intensity of  
 52 mesoscale eddies, contrasting transport of dissolved oxygen, and organic matter (McCreary Jr et al., 2013). Both  
 53 these basins experience intense oxygen depletion below the mixed layer of the water column, where dissolved  
 54 oxygen (DO) is usually below the detection limit of conventional methods. The AS-OMZ between the water  
 55 depths of ~100/150 – 1000/1200m is the thickest OMZ, and is identified as a primary site of fixed nitrogen loss  
 56 (Naqvi et al., 2006). In contrast, in the BoB-OMZ has been reported less intense than the AS-OMZ (Paulmier,  
 57 2009) with DO concentrations still present in the nanomolar range (Bristow et al., 2017). Nitrogen loss has been  
 58 described as rather insignificant and limited by substrate availability resulting from low organic matter supply  
 59 by primary production (Bristow et al., 2017; Löscher et al., 2020). The sequence of electron acceptor utilization  
 60 in such an environment, generally follow the thermodynamic energy yield (Froelich et al., 1979). However,



61 recent studies support the possibility of co-occurrence of metabolisms using different electron acceptors in  
 62 OMZs, one example would be the existence of a cryptic sulfur cycle, which occurs along with nitrogen cycle  
 63 processes (Callbeck et al., 2018; Canfield et al., 2010).

64 Surface sediment underlying OMZs entraps all recent microbial signatures of the water column above  
 65 (Gerdes et al., 2000) in addition to the sediment microbiome; hence it is interesting to explore and compare such  
 66 benthic OMZ ecosystems, especially those located in shallow zones. OMZs act as niches for microorganisms  
 67 that can use alternative pathways of respiration (Diaz and Rosenberg, 2008; Pitcher et al., 2011). In the BoB-  
 68 OMZ, aerobic communities have identified to coexist with anaerobic communities (Bristow et al., 2017). In the  
 69 AS, such coexistence was explained by separate micro-niches in the same environment (Pitcher et al., 2011).  
 70 Similar studies carried out in eastern AS-OMZ sediments have identified Proteobacteria (52%) and  
 71 Planctomycetes (12.7%) as the dominant phyla (Divya et al., 2011). Other integral phyla of soil/sediment habitat  
 72 are Bacteroidetes, Acidobacteria, Actinobacteria, and Firmicutes (Lv et al., 2014).

73 It is vital to understand the dominant microbial taxa and also their functional ecology to throw light on  
 74 the biogeochemistry of these oxygen-depleted zones (Rajpathak et al., 2018). With the advent of molecular  
 75 techniques over the last decade, a large volume of data has been generated which helped to elucidate the  
 76 bacterial community structure (Hodkinson and Grice, 2015). Phylogenetic profiling, using next-generation  
 77 sequencing (NGS) techniques, offer high-resolution data from complex environments (Claesson et al., 2010). By  
 78 using algorithms leveraging functional databases, it is also possible to predict putative functional ecology from  
 79 16S rRNA amplicon data. The available data on the bacterial community structure of the northern Indian Ocean  
 80 OMZ using such high-throughput sequencing techniques has chiefly been limited to the pelagic realm  
 81 (Fernandes et al., 2019; Rajpathak et al., 2018), or restricted to some functionally significant groups rather than  
 82 total bacterial community (Fernandes et al., 2018). Descriptions of OMZ sediment bacterial communities are  
 83 largely underrepresented and need special attention.

84 The objective of our work was to compare the surface sediment bacterial diversity within two major  
 85 OMZs in the northern Indian Ocean, the Arabian Sea (AS) and the Bay of Bengal (BoB), using NGS on the v1-  
 86 v3 hypervariable region of the 16S rRNA gene. Based on this high throughput sequencing dataset, we predicted  
 87 the metabolic potential present at both sites, the AS and the BoB with a key focus on genes relevant for nitrogen  
 88 and sulfur turnover.

89



## 90 2. MATERIALS & METHODS

91

### 92 2.1. Sample collection and site characteristics

93 Sediment samples were collected in February 2013 off Goa in the AS-OMZ (SSK-046, *RV Sindhu*  
 94 *Sankalp*), at the GS1A site located at 15°13'N, 72°56'E, and in August 2014 off Paradip in the BoB (SSD-002,  
 95 *RV Sindhu Sadhana*), at the PS1B site located at 19°57'N, 86°46'E (Fig.1-A). A typical OMZ profile is added  
 96 from the AS and BoB, respectively. Those profiles represent typical conditions for the two sampling locations  
 97 but were obtained from other cruises and show the distribution of dissolved oxygen, nitrate and nitrite from the  
 98 surface to 1000m water depth in  $\mu\text{M}$  (Fig.1-B-C). Sampling at both stations covered surface sediments below a  
 99 ~200m deep water column, underlying OMZ waters. Though both areas experience intense oxygen depletion  
 100 with the core of the OMZ located between 150 and 500 m, the maximum  $\text{NO}_x$  values are twice as high in the AS  
 101 as compared to the BoB, with a prominent secondary nitrite maxima (SNM). A box corer was used to retrieve  
 102 the sediment samples. The sediment cores were carefully sub-sampled using acrylic core liners (25 mm ID, ~30  
 103 cm length), sub-samples were taken from the center of the core to avoid mixing of sediment layers. The 0-5 cm  
 104 subsections of samples were transferred into sterile screw-cap containers. Samples were handled sterile and  
 105 preserved at -20°C until further analysis. The Temperature/Salinity profiling of the water column above the  
 106 sediment was carried out using a Sea-Bird Electronics conductivity-temperature-depth (CTD) sensor (SBE9),  
 107 equipped with a Niskin bottle rosette sampling system, and a dissolved oxygen (DO) sensor (RINKO, ALEC,  
 108 Japan).

109

### 110 2.2. Sediment characterization

111 The sediments were freeze-dried, homogenized, and ground in an agate mortar prior analysis. Total  
 112 carbon (TC) comprising both inorganic and organic carbon, and total nitrogen (TN) comprising dissolved and  
 113 particulate nitrogen and all forms of inorganic nitrogen derivatives were analyzed in an elemental carbon/  
 114 nitrogen (CN) analyzer (FISON NA1500) using the method described in (Bhushan et al., 2001). The  
 115 calibration of the CN analyzer was done using a reference standard (NC-soil), and the obtained recovery rate  
 116 was 96% for TC and 99% for TN. The precision was monitored by carrying out replicates for both samples and  
 117 was  $\pm 1\%$ . The detection limits were two times the blank value. Total organic carbon (TOC) contents were  
 118 determined with a colorimetric based wet oxidation method (Azam and Sajjad, 2005), which is reported to be  
 119 highly reproducible. Inorganic carbon (TIC) was determined as the difference between TC and TOC (Bernard et



al., 1995). Organic matter (OM) was calculated by multiplying TOC with the Van Bemmelen's factor 1.724 (Heaton et al., 2016), based on the assumption that humidified organic matter of soil contains 58% carbon, however, variations of 40-60% have been observed (Nelson and Sommers, 1982). For determining  $\text{CaCO}_3$  abundances, TIC was multiplied with a factor of 8.33 to get the percent calcium carbonate as described previously (Bernard et al., 1995).

### 2.3. Genomic DNA extraction and 454 Pyrosequencing

Total genomic DNA was extracted from 400-500 mg of the sediment samples in triplicates, using the Fast DNA™ SPIN Kit for Soil (MP Biomedicals, Santa Ana, CA). The purified DNA was quantified using a Nanodrop 2000 spectrophotometer (ThermoScientific, USA). DNA was quality checked on an agarose gel (0.8%). The extracted DNA was pooled and amplified using barcoded fusion primers targeting the v1–v3 region of the 16S rRNA gene using the universal primer 9F (AGAGTTTGATCMTGGCTCAG) and 541R (ATTACCGCGGCTGCTGG). Mixed amplicons were subjected to emulsion PCR and then deposited on picotiter plates (Agilent, USA). Amplification conditions consisted of an initial denaturation step at 95°C for 5 min, followed by 30 cycles of denaturation at 95°C for 30 sec, annealing at 55°C for 30 sec, and elongation at 72°C for 30 sec, with a final elongation at 72°C for 5 min. The detailed procedure of pyrosequencing is described elsewhere (Suh et al., 2014). Sequencing was performed by Chunlab Inc. (Seoul, Korea) using a 454 GS FLX Titanium Sequencing system (Roche Branford, CT, USA) per the manufacturer's instructions.

### 2.4. Sequence data processing

Amplicon pyrosequencing data were processed using the QIIME software package, ver. 1.7. (Caporaso et al., 2010). Chimaeras and primer mismatch sequences were removed from the amplicon dataset using the Amplicon Noise software, version 1.27 (Quince et al., 2011) available from the FLX Titanium sequence data platform, and implemented in QIIMEa using the program CD-HIT (Edgar, 2010). The average read length of PCR amplicons was 378±45 bp. The resulting reads were taxonomically classified based on similarity scores in both the basic local search tool (BLASTN) searches ( $E\text{-value} > 10^{-5}$ ) on the EzTaxon-e 16S rDNA database (2014.07.01) and on the SILVA SSU database, release 132, based on the RDP classifier method (version14) (Im et al., 2012). Relative abundances of taxonomic groups were estimated using the following cut-off values: species ( $x \geq 97\%$ ), genus ( $97\% > x \geq 94\%$ ), family ( $94\% > x \geq 90\%$ ), order ( $90\% > x \geq 85\%$ ), class ( $85\% > x \geq 80\%$ ) and phylum ( $80\% > x \geq 75\%$ ). If the similarity was lower than the specific cut-off value, the sequence was



characterized unclassified (un) (Chun et al., 2007); sequences which didn't have any cultivable representatives were shortened as 'ucl.' The diversity indices and rarefaction curves were calculated at 97% sequence similarity using the Mothur platform v.1.43.0. (Schloss et al., 2009). The CLCommunity<sup>TM</sup> software version 3.46 was used for data visualization. Venn diagrams were used to compare sediment bacterial taxonomic composition between sampling sites.

Out of 17,784 reads, 43% were filtered out during the quality processing. After read pre-processing, 5944 reads for the AS sediment, and 4125 reads for the BoB sediment sample were available for further analysis with a mean length of approx. 470-480 bp. In marine sediments, pyrosequencing read numbers varied between 5,000 and 20,000 per sample in previous studies (Zhu et al., 2013;Choi et al., 2016), the output of our sequencing approach is in the same order of magnitude. The taxonomic assignment done using the SILVA platform (Quast et al., 2012) resulted in classifying the bacterial sequences into several specific clades, the EzTaxon-e data analysis (Chun et al., 2007) was used for species-level taxonomic assignment.

## 2.5. Functional prediction of 16S rRNA amplicons

For the functional prediction of 16S rRNA pyrosequencing amplicons, the OTUs were clustered at 97% sequence similarity. The OTU table and representative sequence fasta files were submitted to the Piphillin pipeline (<https://piphillin.secondgenome.com/>) (Iwai et al., 2016). The Piphillin algorithm has the advantage to not rely on phylogenetic trees to predict metagenomic contents. It further uses more recent releases of the functional database Kyoto Encyclopedia of Genes and Genomes (KEGG, updated Oct 2018)) and BioCyc as compared to alternative pipelines such as PICRUSt or Tax4Fun (Narayan et al., 2020). It utilizes nearest-neighbor matching 16S rRNA amplicons (or genomes) to predict the representative genomes. The normalized 16S rRNA copy number of each genome is inferred using gene content collected in functional databases (Langille et al., 2013;Iwai et al., 2016;Narayan et al., 2020).The KEGG reference database was used at a 90% cutoff level to predict metabolic functions present in the sequenced microbial community. The final output of this workflow was quantified in terms of predicted gene abundances per number of OTUs per sample. The information extracted was based a small fraction of the population available from the KEGG database. At 90% similarity cut off, around 338 KEGG pathways were identified from 156 OTU representatives from the AS and 354 KEGG pathways for 469 OTUs from the BoB. We focused on the KEGG database pathways for nitrogen (ko00910), sulfur (ko00920), and methane (ko00680) turnover, as well as on carbon metabolism (ko01200) with specific focus on fermentation and bioenergetics pathway related to carbon fixation.



180

## 181 3. RESULTS AND DISCUSSION

182

### 183 3.1. Sediment biogeochemistry

184 In the present study, both sampling sites showed intense oxygen depletion with dissolved oxygen ( $O_2$ )  
 185 concentrations of  $2 \pm 0.4 \mu M$ . In the shallow zones of BoB-OMZ and in the AS, the  $DO$  concentration  
 186 sometimes falls below the detection limit of conventional methods, especially during the summer monsoon, due  
 187 to the increased riverine nutrient loading, coastal high primary production and increased respiration (Sarma et  
 188 al., 2013). Between both sampling sites, bottom water salinity was comparable, but the temperature differed by  
 189  $3^\circ C$ , which may be a seasonal or permanent feature. The sample characteristics of the collected sediment and  
 190 near-bottom waters are presented in Table 1. In brief, total organic carbon was slightly higher in the AS with  
 191 3.47% and 2.24% in the BoB, TN values were 0.28% and 0.16% in the AS and BoB, respectively. The TOC/TN  
 192 ratio was 8.28 in the AS, and 7.174 in the BoB, thus conditions in the organic matter pool were rather  
 193 comparable. The only striking difference was observed regarding TOC and TN values are in the typical range of  
 194 OMZ sediments and higher than non-OMZ surface sediments with TOC and TN values as low as 0.2 and 0.02  
 195 wt. % (Pattan et al., 2013). OMZs enhance the preservation of organic matter, explaining the reported values of  
 196 TOC ranging from ~1-2 to 6-7% (Cowie et al., 2014) and TOC/TN ratios within 7.3 – 12.3 (van der Weijden et  
 197 al., 1999). Our data is in line with those OMZ-typical ranges, with somewhat lower concentrations for both,  
 198 TOC and TN, in sediments of the BoB. This may result from generally assumed lower productivity of BoB  
 199 waters compared to the AS rapid nitrogen burial as described for OMZ sediments (Robinson et al., 2012), or  
 200 different activities in re-mineralization processes (Bohlen et al., 2011). TIC, which was substantially higher in  
 201 the AS with 8.11%, compared to the BoB with only 0.29%.

202 While in the range of OMZ sediments and higher than the difference in TIC could be attributed to the  
 203 difference in  $CaCO_3$  content caused by increased carbon sequestration (Sarma et al., 2007). Additionally,  
 204 shelled meiobenthic fauna may contribute to the difference in TIC, as this is found to be abundant in sediments  
 205 of the AS while not abundant in the BoB (Ramaswamy and Gaye, 2006). Besides, different microbial  
 206 communities could explain patterns of carbonate precipitation, a possibility which we will explore in the  
 207 following.

208



### 209 3.2. Bacterial diversity in Indian Ocean sediments

210 Between the studied sites, the BoB sediments harbor a more diverse bacterial community than the  
 211 sediments of the AS, which is illustrated not only by the general diversity of taxa and in line with the few  
 212 available other studies (Fig. 3) (Zhu et al., 2013; Dang et al., 2008)) but also corroborated by various diversity  
 213 measures as presented in Table 2. Given that our rarefaction analysis (A1) showed that our sequencing approach  
 214 was able to recover ~70% of bacterial phylotypes from the BoB and 90 % from the AS sediments, the diversity  
 215 in the BoB is however still rather underestimated and may be even higher.

216 The dominant communities and their relative percentage remained the same for BLASTN searches  
 217 using the EzTaxon-e 16S database, where a total of 48 phyla were identified, and pairwise alignment using the  
 218 SILVA 132 database. This led to a successful in classification of 44 phyla, 27 of which were common to both  
 219 sites. Generally, the dominant bacterial phyla consisted of Firmicutes (33.08%), Proteobacteria (32.59%),  
 220 Bacteroidetes (17.48%), and Chloroflexi (5.52%) in AS sediments and Proteobacteria (52.65%),  
 221 Planctomycetes (9.36%), Actinobacteria (7.25%), Firmicutes (5.5%) Acidobacteria (6.74%) and Chloroflexi  
 222 (4.49%) in BoB sediments. Those abundant taxa contributed with >85% to the total bacterial community.

223 The dominance of Proteobacteria is well documented in marine ecosystems (Wang et al., 2012). In the  
 224 eastern AS-OMZ surface sediment, nearly 14 phyla were identified in a previous study using the Sanger  
 225 sequencing technique, the majority of which were Proteobacteria (52%), followed by Planctomycetes (12.7%)  
 226 and Chloroflexi (8.8%) (Divya et al., 2011). Similarly, in another study carried out utilizing high-throughput  
 227 sequencing confirms Proteobacteria to be the dominant phylum making up 70-75% in all six sites within benthic  
 228 OMZ of AS followed by Bacteroidetes. Representative sequences affiliated to phyla Chloroflexi and Firmicutes  
 229 were also recovered in a considerable number (Fernandes et al., 2018). From sediments collected from off  
 230 Paradip port, which is roughly 27 nautical miles from our BoB sampling site PS1B, close to 40 bacterial phyla  
 231 were reported using high-throughput methods similar to our study. The relative contribution of the phylum  
 232 Proteobacteria was only 17%, which was lesser than Bacteroidetes (23%) and Firmicutes (19%) (Pramanik et  
 233 al., 2016) indicating a certain patchiness in relative abundance but an overall comparability of the bacterial  
 234 community composition in the BoB possibly resulting from factors including DO (Stewart et al., 2012), the  
 235 availability of nutrients or organic carbon determine (Fierer and Jackson, 2006).

236 The candidate phyla GN02, OD1, TM6, TM7, and WS3, were prevalent in ESP (eastern south pacific)  
 237 pelagic OMZ microbiome as well, implying that they have an essential role in OMZ nutrient cycling (Ulloa et  
 238 al., 2013; Ganesh et al., 2014). Candidate phyla GN02, OP3, OP8, were unique to both sampled OMZs





sediments of the northern Indian Ocean. A total of 13 candidate phyla were obtained in our study. The prevalence of such “bacterial dark matter” highlights the need to decipher their coding potential, as they can’t be subjected to functional predictions due to a lack of cultivable representatives.

A complete list of taxa is presented in the Supplementary information A2. Interestingly, only 28.48% of the identified OTUs were shared between the AS and the BoB on the genus level were between (64.29% on the phylum level), leaving 53.10% of unique OTUs in the BoB and 18.42% in the AS (Fig. 2). This suggests that the two sediments, while biogeochemically similar, harbor a largely different bacterial community.

The analysis of 58 bacterial classes recovered from our data set showed that there >50% similarities between the phylotypes at the two site which makes up ~97% of bacteria. The dominant classes in the AS sediment include Bacilli (32.96%), Gammaproteobacteria (18.34%) and Bacteroidia (17.19%). In the BoB sediment, Gamma-, Alpha, and Delta-Proteobacteria (23.68%, 19.01%, 9.26% respectively) were most abundant, followed by Planctomycetacia (6.72%). Those clades together contribute between 60-70% of the total in the BoB sediment. Dominant bacterial orders recovered exclusively from the AS-OMZ include Bacillales (32.94%), majorly Planococcaceae (26.06%). Flavobacteriales (17.14%), and Oceanospirillales (12.85%). In BoB sediments, Steroidobacterales (7.05%) and Rhizobiales (11.03%) form the most dominant groups. Exploring the taxonomy in more detail, relative abundances for fermenting organisms such as Planococcaceae, Flavobacteriaceae, Bacillaceae, Oceanospirillaceae, Rhodobacteraceae, and Vibrionaceae are strikingly higher in the AS sediment compared to the BoB amongst the abundant clusters (abundant >1%; Fig. 3). Those clades are mainly described as heterotroph degraders, mostly able to ferment (Glöckner et al., 1999; Yakimov et al., 2003). The presence of Alcanivoraceae in the AS sediment, and their absence in the sediment of the BoB, could be an important factor in the precipitation of  $\text{CaCO}_3$ , because of their metabolic capability to use ammonification and carbonic anhydrase activity to induce rapid calcium carbonate precipitation (Krause et al., 2018). In the BoB, abundant clades consist mostly of Pseudomonadaceae firstly described in a deep sea sediment from a Japanese trench [clone AB013829, (Yanagibayashi et al., 1999)] and Desulfobacteraceae, both of which are described denitrifier groups. Desulfobacteraceae often use acetate (Dyksma et al., 2018) but are also known to degrade other organic compounds (Kümmel et al., 2015). Besides those clades, different proteobacterial clades were found, as well as the purple non-sulfur bacteria Rhodobacteraceae and Rhodospirillaceae, the latter of which are able to fix molecular nitrogen (Madigan et al., 1984). The double pie-chart provides an overview of both sequenced bacterial communities at the class and family level (Fig. 3).



268 In AS sediments, the most abundant bacterial genus was *Paenisporsarcina* sp. (24.06%), followed by  
 269 *Salegentibacter* sp. (17%), and as per EzTaxon-e database those were closer identified as *Paenisporsarcina*  
 270 *quisquiliarum* and *Salegentibacter mishustinae*. Those groups were followed by *Amphritea* (9.02%),  
 271 *Oceanibulbus* (4.27%), *Alcanivorax* (3.82%), *Photobacterium* (2.76%) and *Salipaludibacillus* (2.61%). All of  
 272 those clades were unique to AS sediment and not present in the BoB sediments. In BoB sediments, the most  
 273 abundant taxa were *Woeseia* (6.98%) and *Gammaproteobacteria\_ucl* (6.5%), with the remaining groups being  
 274 represented with less than 3%.

275 The clade *Woeseiaceae/JTB255* is recognized as the most abundant clade in marine sediment, having a  
 276 cosmopolitan distribution. Moreover, analyzed metagenomes of *JTB255* are known to encode the truncated  
 277 denitrification pathway to nitrous oxide (Mußmann et al., 2017). Since denitrification mediated nitrogen loss is  
 278 reported to be dominant in Arabian Sea OMZ, we expected to get more hits in the analyzed amplicon dataset  
 279 (Ward et al., 2009). Though their occurrence was not detected, few representative sequences of *JTB31* and  
 280 *JTB38* have identified which might have a similar role.

281

### 282 3.3. Predicted functional ecology

283 For a large proportion of the amplicons, functions could not be assigned clearly, which leads to a rather  
 284 conservative, and qualitative instead of quantitative estimate of the metabolic potential present at the two sites.  
 285 The predictive functional profiling of 16S rRNA sequences has identified a high proportion of genes involved in  
 286 methane cycling, as generally typical for sediments underlying OMZ waters (Bertics et al., 2013; Fulweiler et al.,  
 287 2007; Gier et al., 2016), followed by genes involved in sulfur and nitrogen cycling. (Fig. 4). Methane turnover  
 288 rates are rather high in anoxic shelf sediments and are were reported to be correlated with the availability of  
 289 labile organic matter, and concurrent with sulfate reduction (Maltby et al., 2016), explaining the predicted  
 290 abundance of genes involved in methane turnover in our samples. Despite the difference in diversity between  
 291 the two sampling sites, almost all predicted gene functions were identical suggesting an overall similar  
 292 metabolic potential in the two different sediments.

293 Nitrogen cycle: In northern Indian Ocean OMZs, nitrogen cycling is reported to be very active (Naqvi  
 294 et al., 2006). At both our sampling sites, genes coding for major nitrogen cycle pathways including nitrogen  
 295 fixation, dissimilatory nitrate reduction to ammonia (DNRA), nitrification, and denitrification were predicted.  
 296 Interestingly, anammox genes were not predicted for either site despite the presence of planctomycetes in our  
 297 dataset (Fig.7). This may be either due to the low number of species-level identifiable OTUs or to a true absence



of anammox-capable planctomycetes as consistent with OMZ sediments from the seasonally anoxic Eckernförde Bay in the Baltic Sea and sediments underlying the Peruvian OMZ (Dale et al., 2011; Bertics et al., 2013). While generally planctomycetes were in the sequence pool, hits corresponding to anammox planctomycetes were indeed very low at our sampling sites, accounting for 0.03 and 0.3% in the AS and BoB, respectively. A sequencing related bias could, however, have led to an underestimation of *Scalindua*-anammox bacteria as a systematic underrepresentation by sequencing of 16SrDNA v1-v3 regions has been reported (Penton et al., 2006). Specifically, the functional marker gene coding for the hydrazine oxidoreductase was not predicted from our 16S rDNA data. This suggests that the contribution of anammox to the nitrogen cycle in the Indian Ocean sediments, at least at our sampling sites, is rather low similar to the pelagic OMZ of the AS where denitrification is reported to be dominant over anammox (Ward et al., 2009), and the BoB where anammox as well as denitrification could not be detected (Bristow et al., 2017) active. As Planctomycetales are known to encode a large number of sulfatase genes, which makes them as a specialist for the initial breakdown of sulfated hetero-polysaccharides (Wegner et al., 2013), their role in the Indian Ocean sediments could rather be carbon capture in the sediments (Jensen et al., 2011; Arango et al., 2007; Shao et al., 2010; Dale et al., 2011). Here, the predicted gene abundance was 848 and 2901 for AS and BoB microbiome for the predominant form being arylsulfatase, respectively, contributing 65-85% of the sulfatase pool.

The global annual denitrification rate in sediment would be approximately 200 Tg N, and the majority contributed from sediments underlying OMZ, where its reported two to four times higher (Devol, 2015). Therefore, nitrogen loss processes would be expected to take place in both, sediments of the AS and the BoB. Denitrification and sulfite reductase genes were prevalent in our prediction possibly favoring sulfur driven autotrophic denitrification (Shao et al., 2010), and as previous studies suggested heterotrophic denitrification (Arango et al., 2007). Other denitrifiers recovered from our sequence dataset are Oceanospirillales, Chromatiales, Nitrospirales, Syntrophobacteriales, and NB1-j which are known to encode denitrification genes including *nirS*, *norB* and *nosZ* (de Voogd et al., 2015), and contributed 14.05% in the AS sediment, and 4.46% in the BoB sediment, respectively. Similarly, Flavobacteriales are known denitrifiers (Horn et al., 2005), and was are abundant in the AS with 17.14% of all 16S rDNA sequences.

Recent studies have also linked methane oxidation to nitrite-based denitrification in the Candidatus phylum NC10 (Padilla et al., 2016). This was supported by studies carried out in a freshwater reservoir, where methane stimulated massive nitrogen loss (Naqvi et al., 2018). As denitrification is reported to be dominated over anammox in the northern Indian Ocean OMZ (Ward et al., 2009), and our data confirm the same for Indian



328 Ocean sediments, the coupling of methane oxidation and denitrification might be a possible nitrogen loss  
 329 pathway. Identified, *Steroidobacter* clades, which are known to perform denitrification coupled with methane  
 330 oxidation (Liu et al., 2014), make up 7% of the BoB-OMZ bacterial community.

331 DNRA was predicted as a potential pathway in both basins of our study. In seasonally hypoxic Baltic  
 332 Sea sediments, DNRA accounted for almost 75% of benthic nitrogen flux (Dale et al., 2011). In contrast to the  
 333 other nitrogen cycle genes, the *nifHDK* operon coding for the functional unit of the key gene for nitrogen  
 334 fixation, the nitrogenase, was predicted in higher abundance in the BoB compared to the AS, with BoB-nif  
 335 being five times as many as AS-nif. This is consistent with the higher proportions of known sedimentary  
 336 nitrogen fixers, such as *Desulfobacteraceae* and *Rhodospirillaceae*. The presence of nitrogen fixers in sediments  
 337 underlying OMZs has been documented for several regions, including the upwelling system off Mauretania, the  
 338 Baltic Sea and the eastern tropical South Pacific shelves, and nitrogen fixing microbes have been shown to be  
 339 active although at low rates (Bertics et al., 2013; Gier et al., 2017; Gier et al., 2016).

340 Sulfur cycling: For the sulfur cycle in both, the AS and the BoB, genes for the assimilatory pathway of  
 341 sulfate reduction were predicted, as well as sulfur oxidation genes of the *sox* operon (Fig.8) in line with a  
 342 previous study which identified diverse sulfur reducing bacterial and archaeal OTUs in the AS (Fernandes et al.,  
 343 2018). In our AS dataset, a potential player in the sulfur cycle could be *Sulfitobacter dubius*, which was  
 344 represented with 4.32% of all OTUs. All known species of the genus *Sulfitobacter* were isolated from marine  
 345 habitats and are known to perform sulfite oxidation (Sorokin, 1995; Long et al., 2011). *Thermodesulfobrevibrio*  
 346 (phylum Nitrospira) accounted for ~1% of sequences at both sites are known sulfate reducers and have been  
 347 identified from the eastern tropical South Pacific OMZ, before (Schunck et al., 2013). Sequences corresponding  
 348 to sulfur reducers like *Desulfobacterales* (AS: 0.87%, BoB: 2.57%) and *Syntrophobacterales* (AS: 0.67%, BoB:  
 349 1.21%) were also recovered from our dataset and were shown to be abundant in sediments of the Black Sea  
 350 sulfate-methane transition zone as well as in the Arabian Sea OMZ in both pelagic and benthic realms  
 351 (Fernandes et al., 2018; Fuchs et al., 2005; Leloup et al., 2007).

352 Carbon fixation: In the BoB sediment, around 1.75% of gene families were predicted to perform  
 353 photosynthesis, and major contributors would possibly be *Chromatiales* (07%), *Rhodospirillales* (0.03%), and  
 354 members of phylum *Cyanobacteria* (1.65%). *Chromatiales*, a group of purple sulfur bacteria, can perform  
 355 anoxygenic photosynthesis (Manske et al., 2005). Similarly, *Rhodospirillales* primarily chemoorganotroph and  
 356 photoheterotroph (Luo and Moran, 2015), can also perform anoxygenic photosynthesis (Manske et al., 2005).  
 357 It's interesting to note that around 68 *Cyanobacterial* sequences were retrieved from BoB sediment, where water



column depth was ~245m, but only one representative from the AS sediment, which was located at ~200m depth. In addition, in the AS sediment, we observed Chroococcales, which are assumed to be a low-light adapted group (West et al., 2001). The key enzymes responsible for energy metabolism are presented in Table-3. In particular, the higher predicted abundance of dehydrogenase enzymes responsible for oxidation of organic matter in the AS points towards a difference in carbon metabolism in the two regions. This is most likely due to the increased availability of carbon in the AS, however, as proposed earlier (Orsi et al., 2017), more efficient organic carbon recycling in the AS may over geological timescales contribute to developing a stronger and more persistent functional anoxia.

Carbon remineralization: As indicated by the high TIC concentration in the AS sediment, carbon remineralization was very active due to the increased availability of organic carbon (Yu et al., 2018). About 20% of the identified bacteria were common soil/sediment inhabitants with a prime role is remineralization of diverse organic carbon compounds (Schimel and Schaeffer, 2015). These include Acidobacteria, Actinobacteria, Bacteroidetes, and Gemmatimonadetes (Janssen, 2006). Similarly, Anaerolineales (phylum Chloroflexi), which contributed 2-3% of the total hits in our dataset, have also been identified with a similar role and were specific to areas that show very low or zero oxygen. In addition, genes responsible for N-glycan degradation (ko00511) were predicted to occur almost twelve times more often in the AS than in the BoB sample. These genes play a role in cell adhesion and sequestration (Varki and Gagneux, 2017). The relative distribution of key enzymes and genes specific to gram-positive and gram-negative bacterial fermenters were compared based on previous reports (Ramos et al., 2000; Eschbach et al., 2004) (Fig.6). Their predicted abundance was higher in AS sediment than in BoB sediments. The connected more complete carbon remineralization which could add an explanation to why the AS-OMZ is more anoxic than the BoB-OMZ as previously suggested (Orsi et al).

#### 4. CONCLUSION

We compared bacterial communities from two sites in the northern Indian Ocean OMZ, in the BoB off Paradip and a site off Goa in the AS. Less than one-third of the phylotypes were shared between the two sites, leaving a large individual proportion of the bacteria for each site. A higher diversity has been identified from the BoB, compared to the AS, however, our functional prediction identified high abundances of typical heterotrophic degraders in the AS, that were only represented in low proportions or absent in the BoB. We further identified denitrifiers, DNRA bacteria and sulfur cycle bacteria at both sites and predicted the presence



of their functional genes. The higher functional diversity for organic matter degradation with fermentation in addition to denitrification and sulfur-compound dependent remineralization may explain, why the AS OMZ is generally more anoxic. Here, the variability in carbon respiration pathways may allow for a more efficient or complete respiration along the electron tower, thus consuming more oxidized compounds. The abundance of Alcanivorax-like bacteria in AS sediments may provide an explanation for high CaCO<sub>3</sub> precipitation, as this organism has been described to perform this process rapidly when organic nitrogen is available as it is at our sampling site in the AS. A notable finding was the absence of anammox bacteria at both sites. Notably, we predicted nitrogen fixation genes from BoB sediments but not from AS sediments, possibly resulting from higher nitrogen inputs from the water column in the AS.

Despite the limitation of this study with regard to our sample number, we could contribute a first assessment of bacterial diversity and functionality in coastal sediments of the two Indian Ocean basins, as such, we hope to contribute to the general understanding of how these basins work and why they are so different in their biogeochemistry.

#### DATA AVAILABILITY

All pyrosequencing reads were submitted to the NCBI Genebank database under accession number KU821783 - KU831324 and MG860544 - MG860851. The supporting information is available as supplementary information.

#### APPENDICES

**A1:** Rarefaction curve of bacterial OTUs (operational taxonomic units) associated with sediments underlying oxygen-depleted waters in the northern Indian Ocean OMZ.

**A2:** Taxonomic composition of bacterial OTUs analyzed through the SILVA database.

#### AUTHOR CONTRIBUTION

JL prepared the manuscript and performed the experiments and bioinformatics analysis. CSM conceived the idea and designed the experiment.

#### COMPETING INTERESTS

The authors declare that they have no conflict of interest.



418

419 **FUNDING**

420 The first author is grateful to the Council of Scientific and Industrial Research (CSIR), India, for  
421 fellowship grant 31/026(0245)/2012-EMR-I for doing a Ph.D. This work is supported by CSIR grant: PSC0108.  
422 NIO's contribution no: xxxx.

423

424 **ACKNOWLEDGMENT**

425 We thank the Director of CSIR-NIO for providing the facilities. We acknowledge Chun Lab, Seoul,  
426 South Korea, for carrying out pyrosequencing. Special thanks to Dr. Carolin Löscher for the critical comments  
427 and valuable suggestions which have significantly helped in improvising the content. We express our gratitude  
428 to Dr. Amal Jayakumar, Dr. N. Ramaiah and Dr. Peter Burkill for guidance in manuscript preparation. We also  
429 thank crew members of SSK-046 and SSD-002, especially Ms. Larissa Menezes, for GS1A sample collection.

430

431



## 432 LEGENDS

433

434 **Table 1:** Sediment and bottom water characteristics for the samples collected from the northern Indian Ocean  
 435 OMZ.

436 **Table 2:** Summary of pyrosequencing results and statistical analysis of bacterial sequences retrieved from the  
 437 northern Indian Ocean OMZ surface sediment samples.

438 \*OTUs (operational taxonomic unit) were calculated using Mothur (3% distance).

439 §Good's coverage is proportional to non-singleton phylotypes.

440 **Table 3:** Distribution of key enzymes relevant in energy metabolism in the northern Indian Ocean surface  
 441 sediments predicted from 16S rRNA genes.

442

443 **Fig. 1:** A) Station map, blue dots indicate sampling stations, red dots are the regions where OMZ water-column  
 444 characteristics were obtained from. B) Representative water column profiles of biogeochemical parameters from  
 445 (B) the AS-OMZ (Unpublished data, personal communication from Dr. G.V.M. Gupta) and C) the BoB- OMZ  
 446 (Sarma et al., 2013).

447 **Fig. 2:** Venn diagram showing OTU number wise comparison of the phylotypes at different taxonomic level  
 448 assigned through the SILVA database.

449 **Fig. 3:** Dominant bacterial taxa retrieved at 1% cut-off based on pairwise alignment in the SILVA SSU database  
 450 release 132.

451 **Fig. 4:** Double Pie chart showing bacterial community composition at the class and family level from the  
 452 sampling locations based on the EzTaxon-e database.

453 **Fig. 5:** Relative distribution of redox metabolic KEGG pathways identified from our 16S rRNA amplicon  
 454 pyrosequencing dataset utilizing the Piphillin algorithm.

455 **Fig. 6:** Percentage distribution of key enzymes with coding genes identified in bacterial fermentation (Ramos et  
 456 al., 2000; Eschbach et al., 2004).

457 **Fig. 7:** Proposed pathway for OMZ Nitrogen cycling in sediments of northern Indian Ocean OMZ, and the  
 458 abundance of enzymes with coding genes are indicated in box, where 'blue' and 'red' denotes AS and BoB gene  
 459 count. Expansion of abbreviation are as follows:- **amoA**: Ammonia monooxygenase subunit A; **gdh**: Glutamate  
 460 dehydrogenase; **hao**: Hydroxylamine oxidoreductase; **hzo**: Hydrazine oxidoreductase; **hzs**: Hydrazine synthase;  
 461 **napA**: Nitrate reductase (cytochrome); **nasA**: Nitrate reductase; **narG**: Nitrate reductase, alpha subunit; **nifH**:





462 Nitrogenase iron protein; **nirK/nirS**: Nitrite reductase subunit K/S; **norB/norC**: Nitric oxide reductase subunit  
 463 B/C; **nrfA**: nitrite reductase (cytochrome c-552); **nosZ**: Nitrous oxide reductase; **nrxA**: nitrite oxidoreductase,  
 464 alpha subunit; **ureC**: Urease subunit alpha.

465 **Fig. 8:** Proposed pathway for OMZ Sulfur cycling in sediments of northern Indian Ocean OMZ, and the  
 466 abundance of enzymes with coding genes are indicated in box, where 'blue' and 'red' denotes AS and BoB gene  
 467 count. Expansion of abbreviation are as follows:- **aprA**: Adenylylsulfate reductase, subunit A; **dsrA/dsrB**:  
 468 Dissimilatory sulfite reductase subunit-alpha/beta; **dsrC**: Dissimilatory sulfite reductase related protein; **cysC**:  
 469 Adenylylsulfate kinase; **cysH**: Phosphoadenosine phosphosulfate reductase; **psrA**: Thiosulfite reductase; **rDsr**:  
 470 Reverse dissimilatory sulfite reductase; **sat**: Sulfate adenylyltransferase; **soeA**: Sulfite:quinone oxidoreductase;  
 471 **sir**: Sulfite reductase (ferredoxin); **soxB**: S-sulfosulfanyl-L-cysteine sulfohydrolase; **soxC**: Sulfane  
 472 dehydrogenase; **soxD**: S-disulfanyl-L-cysteine oxidoreductase; **soxX/A**: L-cysteine S-thiosulfotransferase;  
 473 **soxY/Z**: Sulfur-oxidizing protein; **sseA**: Thiosulfate/3-mercaptopyruvate sulfurtransferase; **sqr**: Sulfide:quinone  
 474 oxidoreductase; .

475

476

477

478

479

480

481

482

483

484

485

486

487



## 488 TABLES

489 **Table 1**

Sampling Details			Sediment Characteristics						Near-bottom water profile (CTD)		
Station code	Date	Sampling depth	TOC	TIC	TN	CaCO3	OM	TOC/T N	DO	Temp	Salinity
			%						μM	°C	PSU
GS1A	Feb-2013	200m	2.012	8.11	0.28	67.556	3.469	7.174	2.313	15.584	35.345
PS1B	Aug-2014	244m	1.297	0.289	0.157	2.407	2.236	8.279	1.666	12.326	35.018

490

491 **Table 2**

Sample name	Optimized reads	OTU richness*				OTU diversity*		Good's coverage§
		Observed	Chao1	ACE	Jackknife	Shannon	Simpson	
GS1A	5,944	955	2,506	4,305	3,450	4.37	0.934	0.893
PS1B	4,125	1,889	4,447	7,616	6,242	6.97	0.998	0.695

492

493 **Table 3**

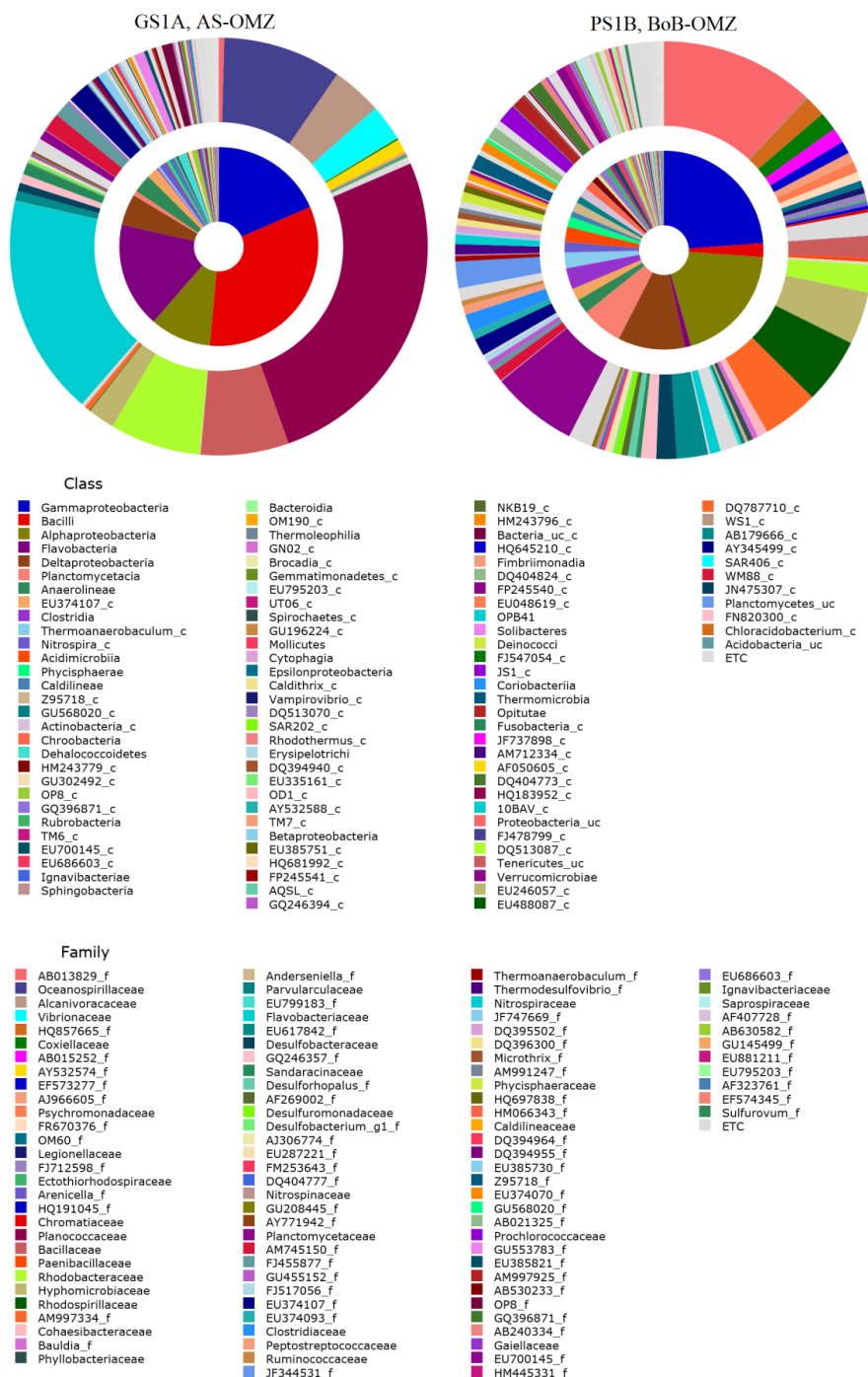
ENERGY METABOLISM	KEGG	ENZYMES	GS1A	PS1B
Kreb cycle, NADH+H <sup>+</sup>	K00161	pyruvate dehydrogenase E1 component alpha subunit [EC:1.2.4.1]	836	454
Kreb cycle, NADH+H <sup>+</sup>	K00627	pyruvate dehydrogenase E2 component (dihydrolipoamide acetyltransferase) [EC:2.3.1.12]	1279	1108
Kreb cycle, NADH+H <sup>+</sup>	K00382	dihydrolipoamide dehydrogenase [EC:1.8.1.4]	2476	1889
Kreb cycle, NADH+H <sup>+</sup>	K00031	isocitrate dehydrogenase [EC:1.1.1.42]	993	1345
Kreb cycle, NADH+H <sup>+</sup>	K00164	2-oxoglutarate dehydrogenase E1 component [EC:1.2.4.2]	895	850
Kreb cycle, GTP	K01902	succinyl-CoA synthetase alpha subunit [EC:6.2.1.5]	1064	952
Kreb cycle, FADH <sub>2</sub>	K00239	succinate dehydrogenase / fumarate reductase, flavoprotein subunit [EC:1.3.5.1 1.3.5.4]	902	906
Kreb cycle, NADH+H <sup>+</sup>	K00024	malate dehydrogenase [EC:1.1.1.37]	1051	881
Glycolysis, ATP	K00927	phosphoglycerate kinase [EC:2.7.2.3]	898	953
Glycolysis, ATP	K00873	pyruvate kinase [EC:2.7.1.40]	955	1012
Glycolysis, NADH+H <sup>+</sup>	K00134	glyceraldehyde 3-phosphate dehydrogenase [EC:1.2.1.12]	2125	1176
Glyoxylate cycle, NADH+H <sup>+</sup>	K00024	malate dehydrogenase [EC:1.1.1.37]	1051	881
Glyoxylate cycle, FADH <sub>2</sub>	K00240	succinate dehydrogenase / fumarate reductase, iron-sulfur subunit [EC:1.3.5.1 1.3.5.4]	916	926
Pentose phosphate pathway, NADPH	K00036	glucose-6-phosphate 1-dehydrogenase [EC:1.1.1.49 1.1.1.363]	678	856
Pentose phosphate pathway, NADPH	K00033	6-phosphogluconate dehydrogenase [EC:1.1.1.44 1.1.1.343]	823	807
Ethylmalonyl pathway, NADP <sup>+</sup>	K14446	crotonyl-CoA carboxylase/reductase [EC:1.3.1.85]	230	276
Ethylmalonyl pathway, GTPase activity	K01847	methylmalonyl-CoA mutase [EC:5.4.99.2]	1386	669
Ethylmalonyl pathway, NADP <sup>+</sup>	K00023	acetoacetyl-CoA reductase [EC:1.1.1.36]	309	345
Ethylmalonyl pathway, ADP +Pi	K01965	propionyl-CoA carboxylase alpha chain [EC:6.4.1.3]	575	329
Ethylmalonyl pathway, ADP +Pi	K01966	propionyl-CoA carboxylase beta chain [EC:6.4.1.3 2.1.3.15]	746	351
Malonate semialdehyde pathway, ADP+Pi	K01961	acetyl-CoA carboxylase, biotin carboxylase subunit [EC:6.4.1.2 6.3.4.14]	1212	938
Propanoyl-CoA metabolism, ADP+Pi	K01965	propionyl-CoA carboxylase alpha chain [EC:6.4.1.3]	575	329





501 Fig. 3

502



503



Fig. 4

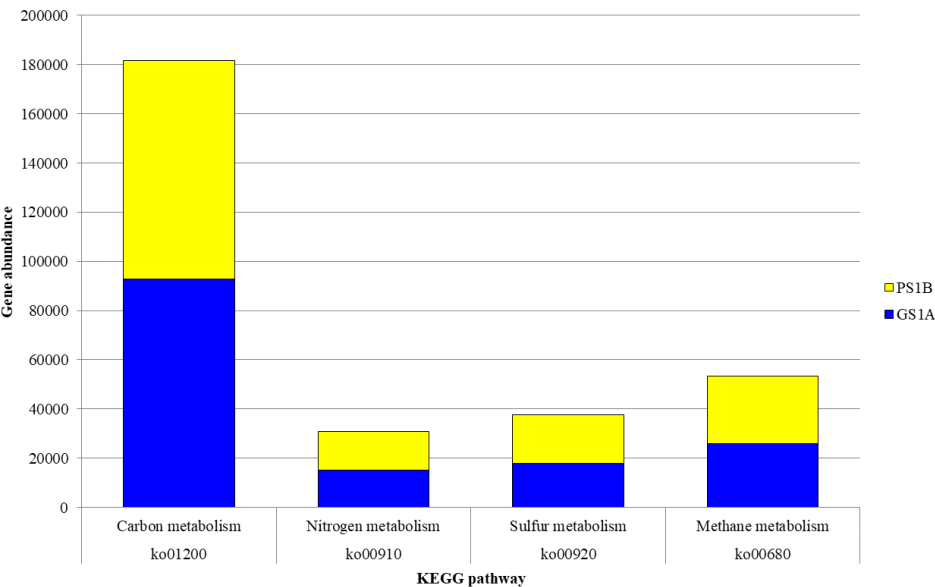


Fig. 5

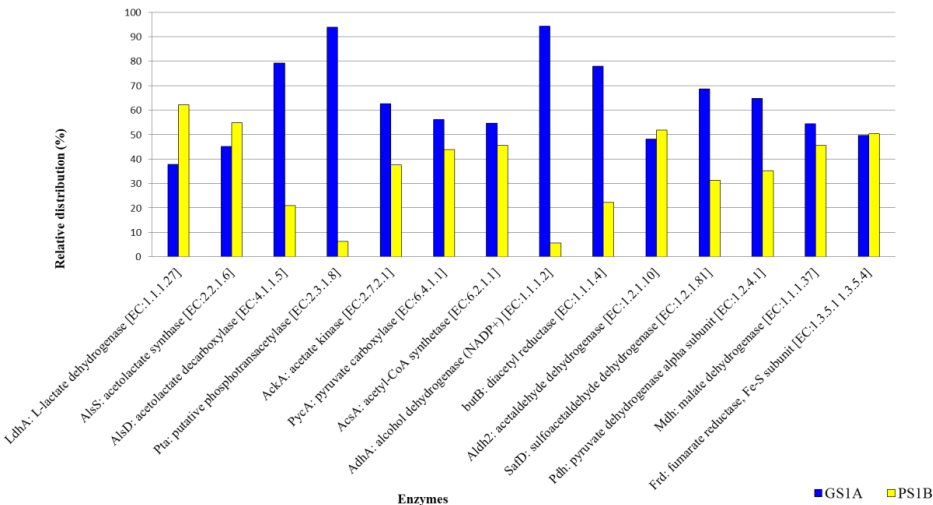
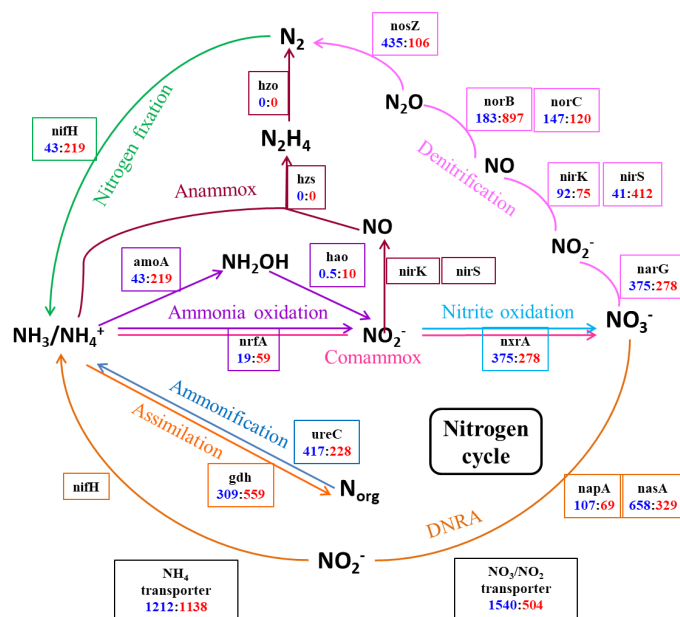


Fig. 6



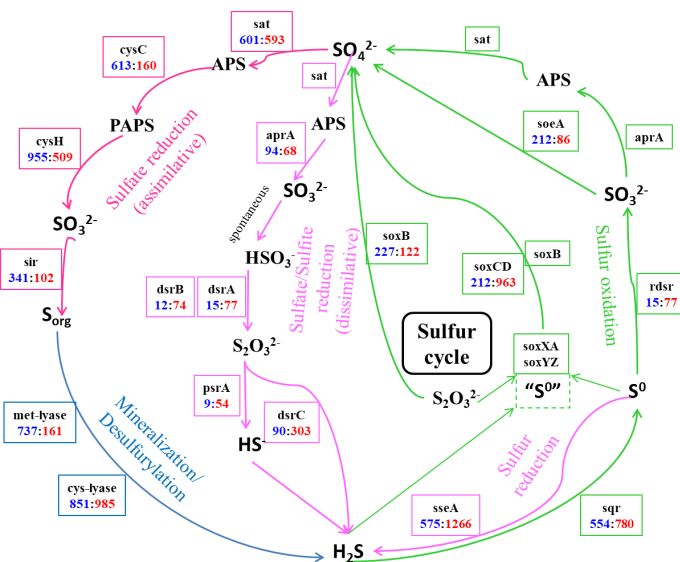
512

513



514

515 Fig. 7



516

517 Fig. 8

518



## 519 REFERENCES:

- 520 Arango, C. P., Tank, J. L., Schaller, J. L., Royer, T. V., Bernot, M. J., and David, M. B.: Benthic organic carbon  
 521 influences denitrification in streams with high nitrate concentration, *Freshw. Biol.*, 52, 1210-1222,  
 522 doi:10.1111/j.1365-2427.2007.01758.x, 2007.
- 523 Azam, F., and Sajjad, M.: Colorimetric determination of organic carbon in soil by dichromate digestion in a  
 524 microwave oven, *Pak. J. Biol. Sci.*, 8, 596-598, doi:10.3923/pjbs.2005.596.598, 2005.
- 525 Bernard, B. B., Bernard, H., and Brooks, J. M.: Determination of total carbon, total organic carbon and  
 526 inorganic carbon in sediments. In: TDI-Brooks International/B&B Laboratories Inc. College Station, Texas,  
 527 1995.
- 528 Bertics, V. J., Löscher, C. R., Salonen, I., Dale, A. W., Gier, J., Schmitz, R. A., and Treude, T.: Occurrence of  
 529 benthic microbial nitrogen fixation coupled to sulfate reduction in the seasonally hypoxic Eckernförde Bay,  
 530 Baltic Sea, *Biogeosciences*, 10, 1243-1258, doi:10.5194/bg-10-1243-2013, 2013.
- 531 Bhushan, R., Dutta, K., and Somayajulu, B.: Concentrations and burial fluxes of organic and inorganic carbon  
 532 on the eastern margins of the Arabian Sea, *Mar. Geol.*, 178, 95-113, doi:10.1016/S0025-3227(01)00179-7,  
 533 2001.
- 534 Bohlen, L., Dale, A. W., Sommer, S., Mosch, T., Hensen, C., Noffke, A., Scholz, F., and Wallmann, K.: Benthic  
 535 nitrogen cycling traversing the Peruvian oxygen minimum zone, *Geochim. Cosmochim. Acta.*, 75, 6094-6111,  
 536 doi:10.1016/j.gca.2011.08.010, 2011.
- 537 Bristow, L. A., Callbeck, C. M., Larsen, M., Altabet, M. A., Dekaezemacker, J., Forth, M., Gauns, M., Glud, R.  
 538 N., Kuypers, M. M., and Lavik, G.: N<sub>2</sub> production rates limited by nitrite availability in the Bay of Bengal  
 539 oxygen minimum zone, *Nat. Geosci.*, 10, 24-29, doi:10.1002/lom3.10126, 2017.
- 540 Callbeck, C. M., Lavik, G., Ferdelman, T. G., Fuchs, B., Gruber-Vodicka, H. R., Hach, P. F., Littmann, S.,  
 541 Schoffelen, N. J., Kalvelage, T., and Thomsen, S.: Oxygen minimum zone cryptic sulfur cycling sustained by  
 542 offshore transport of key sulfur oxidizing bacteria, *Nat. Commun.*, 9, 1729-1740, doi:10.1038/s41467-018-  
 543 04041-x, 2018.
- 544 Canfield, D. E., Stewart, F. J., Thamdrup, B., De Brabandere, L., Dalsgaard, T., Delong, E. F., Revsbech, N. P.,  
 545 and Ulloa, O.: A cryptic sulfur cycle in oxygen-minimum-zone waters off the Chilean coast, *Science*, 330,  
 546 1375-1378, doi:10.1126/science.1196889, 2010.
- 547 Caporaso, J. G., Kuczynski, J., Stombaugh, J., Bittinger, K., Bushman, F. D., Costello, E. K., Fierer, N., Peña,  
 548 A. G., Goodrich, J. K., and Gordon, J. I.: QIIME allows analysis of high-throughput community sequencing  
 549 data, *Nat. Methods*, 7, 335-336, doi:10.1038/nmeth.f.303, 2010.
- 550 Choi, H., Koh, H.-W., Kim, H., Chae, J.-C., and Park, S.-J.: Microbial community composition in the marine  
 551 sediments of Jeju Island: next-generation sequencing surveys, *J Microbiol Biotechnol*, 26, 883-890,  
 552 doi:10.4014/jmb.1512.12036, 2016.
- 553 Chun, J., Lee, J.-H., Jung, Y., Kim, M., Kim, S., Kim, B. K., and Lim, Y.-W.: EzTaxon: a web-based tool for  
 554 the identification of prokaryotes based on 16S ribosomal RNA gene sequences, *Int. J. Syst. Evol. Microbiol.*, 57,  
 555 2259-2261, doi:10.1099/ijs.0.64915-0, 2007.
- 556 Claesson, M. J., Wang, Q., O'Sullivan, O., Greene-Diniz, R., Cole, J. R., Ross, R. P., and O'Toole, P. W.:  
 557 Comparison of two next-generation sequencing technologies for resolving highly complex microbiota  
 558 composition using tandem variable 16S rRNA gene regions, *Nucleic Acids Res.*, 38, e200,  
 559 doi:10.1093/nar/gkq873, 2010.
- 560 Cowie, G., Mowbray, S., Kurian, S., Sarkar, A., White, C., Anderson, A., Vergnaud, B., Johnstone, G., Brear,  
 561 S., and Woulds, C.: Comparative organic geochemistry of Indian margin (Arabian Sea) sediments: estuary to  
 562 continental slope, *Biogeosciences*, 11, 6683-6696, doi:10.5194/bg-11-6683-2014, 2014.
- 563 Dale, A. W., Sommer, S., Bohlen, L., Treude, T., Bertics, V. J., Bange, H. W., Pfannkuche, O., Schorp, T.,  
 564 Mattsdotter, M., and Wallmann, K.: Rates and regulation of nitrogen cycling in seasonally hypoxic sediments  
 565 during winter (Boknis Eck, SW Baltic Sea): Sensitivity to environmental variables, *Estuar. Coast. Shelf Sci.*, 95,  
 566 14-28, doi:10.1016/j.ecss.2011.05.016, 2011.
- 567 Dang, H., Zhang, X., Sun, J., Li, T., Zhang, Z., and Yang, G.: Diversity and spatial distribution of sediment  
 568 ammonia-oxidizing crenarchaeota in response to estuarine and environmental gradients in the Changjiang  
 569 Estuary and East China Sea, *Microbiology*, 154, 2084-2095, doi:10.1099/mic.0.2007/013581-0, 2008.



- 570 de Voogd, N. J., Cleary, D. F., Polónia, A. R., and Gomes, N. C.: Bacterial community composition and  
 571 predicted functional ecology of sponges, sediment and seawater from the thousand islands reef complex, West  
 572 Java, Indonesia, FEMS Microbiol. Ecol., 91, fiv019, doi:10.1093/femsec/fiv019, 2015.
- 573 Devol, A. H.: Denitrification, anammox, and  $N_2$  production in marine sediments, Annu. Rev. Mar. Sci., 7, 403-  
 574 423, doi:10.1146/annurev-marine-010213-135040, 2015.
- 575 Diaz, R. J., and Rosenberg, R.: Spreading dead zones and consequences for marine ecosystems, Science, 321,  
 576 926-929, doi:10.1126/science.1156401, 2008.
- 577 Divya, B., Parvathi, A., Bharathi, P. L., and Nair, S.: 16S rRNA-based bacterial diversity in the organic-rich  
 578 sediments underlying oxygen-deficient waters of the eastern Arabian Sea, World J. Microbiol. Biotechnol., 27,  
 579 2821-2833, doi:10.1007/s11274-011-0760-0, 2011.
- 580 Dykma, S., Lenk, S., Sawicka, J. E., and Mußmann, M.: Uncultured Gammaproteobacteria and  
 581 Desulfobacteraceae Account for Major Acetate Assimilation in a Coastal Marine Sediment, Front. Microbiol., 9,  
 582 3124-3124, doi:10.3389/fmicb.2018.03124, 2018.
- 583 Edgar, R. C.: Search and clustering orders of magnitude faster than BLAST, Bioinformatics, 26, 2460-2461,  
 584 doi:10.1093/bioinformatics/btq461, 2010.
- 585 Eschbach, M., Schreiber, K., Trunk, K., Buer, J., Jahn, D., and Schobert, M.: Long-term anaerobic survival of  
 586 the opportunistic pathogen *Pseudomonas aeruginosa* via pyruvate fermentation, J. Bacteriol, 186, 4596-4604,  
 587 doi:10.1128/JB.186.14.4596-4604.2004, 2004.
- 588 Fernandes, G. L., Shenoy, B. D., Menezes, L. D., Meena, R. M., and Damare, S. R.: Prokaryotic Diversity in  
 589 Oxygen Depleted Waters of the Bay of Bengal Inferred Using Culture-Dependent and-Independent Methods,  
 590 Indian J. Microbiol., 59, 193-199, doi:10.1007/s12088-019-00786-1, 2019.
- 591 Fernandes, S., Mazumdar, A., Bhattacharya, S., Peketi, A., Mapder, T., Roy, R., Carvalho, M. A., Roy, C.,  
 592 Mahalakshmi, P., and Da Silva, R.: Enhanced carbon-sulfur cycling in the sediments of Arabian Sea oxygen  
 593 minimum zone center, Sci. Rep., 8, 8665-8680, doi:10.1038/s41598-018-27002-2, 2018.
- 594 Fierer, N., and Jackson, R. B.: The diversity and biogeography of soil bacterial communities, Proc. Natl. Acad.  
 595 Sci. U. S. A., 103, 626-631, doi:10.1016/j.apsoil.2019.06.008, 2006.
- 596 Froelich, P. N., Klinkhammer, G., Bender, M. a. a., Luedtke, N., Heath, G. R., Cullen, D., Dauphin, P.,  
 597 Hammond, D., Hartman, B., and Maynard, V.: Early oxidation of organic matter in pelagic sediments of the  
 598 eastern equatorial Atlantic: suboxic diagenesis, Geochim. Cosmochim. Acta, 43, 1075-1090, doi:10.1016/0016-  
 599 7037(79)90095-4, 1979.
- 600 Fuchs, B. M., Woebken, D., Zubkov, M. V., Burkill, P., and Amann, R.: Molecular identification of  
 601 picoplankton populations in contrasting waters of the Arabian Sea, Aquat. Microb. Ecol., 39, 145-157,  
 602 doi:10.3354/ame039145, 2005.
- 603 Fulweiler, R. W., Nixon, S. W., Buckley, B. A., and Granger, S. L.: Reversal of the net dinitrogen gas flux in  
 604 coastal marine sediments, Nature, 448, 180-182, doi:10.1038/nature05963, 2007.
- 605 Ganesh, S., Parris, D. J., DeLong, E. F., and Stewart, F. J.: Metagenomic analysis of size-fractionated  
 606 picoplankton in a marine oxygen minimum zone, ISME J., 8, 187-211, doi:10.1038/ismej.2013.144, 2014.
- 607 Gerdes, G., Klenke, T., and Noffke, N.: Microbial signatures in peritidal siliciclastic sediments: a catalogue,  
 608 Sedimentology, 47, 279-308, doi:10.1046/j.1365-3091.2000.00284.x, 2000.
- 609 Gier, J., Sommer, S., Löscher, C. R., Dale, A. W., Schmitz, R. A., and Treude, T.: Nitrogen fixation in  
 610 sediments along a depth transect through the Peruvian oxygen minimum zone, Biogeosciences, 13, 4065-4080,  
 611 doi:10.5194/bg-13-4065-2016, 2016.
- 612 Gier, J., Löscher, C. R., Dale, A. W., Sommer, S., Lomnitz, U., and Treude, T.: Benthic Dinitrogen Fixation  
 613 Traversing the Oxygen Minimum Zone Off Mauritania (NW Africa), Front. Mar. Sci., 4,  
 614 doi:10.3389/fmars.2017.00390, 2017.
- 615 Glöckner, F. O., Fuchs, B. M., and Amann, R.: Bacterioplankton compositions of lakes and oceans: a first  
 616 comparison based on fluorescence in situ hybridization, Environ Microbiol., 65, 3721-3726,  
 617 doi:10.1128/aem.65.8.3721-3726., 1999.
- 618 Heaton, L., Fullen, M. A., and Bhattacharyya, R.: Critical analysis of the van Bemmelen conversion factor used  
 619 to convert soil organic matter data to soil organic carbon data: Comparative analyses in a UK loamy sand soil,  
 620 Espaço Aberto, 6, 35-44, doi:10.36403/espacoaberto.2016.5244, 2016.





- 621 Hodkinson, B. P., and Grice, E. A.: Next-generation sequencing: a review of technologies and tools for wound  
622 microbiome research, *Adv. Wound Care*, 4, 50-58, doi:10.1089/wound.2014.0542, 2015.
- 623 Horn, M. A., Ihssen, J., Matthies, C., Schramm, A., Acker, G., and Drake, H. L.: *Dechloromonas denitrificans*  
624 sp. nov., *Flavobacterium denitrificans* sp. nov., *Paenibacillus anaericanus* sp. nov. and *Paenibacillus terrae*  
625 strain MH72, N<sub>2</sub>O-producing bacteria isolated from the gut of the earthworm *Aporrectodea caliginosa*, *Int. J.*  
626 *Syst. Evol. Microbiol.*, 55, 1255-1265, doi:10.1099/ijs.0.63484-0, 2005.
- 627 Im, W.-T., Hu, Z.-Y., Kim, K.-H., Rhee, S.-K., Meng, H., Lee, S.-T., and Quan, Z.-X.: Description of  
628 *Fimbriimonas ginsengisoli* gen. nov., sp. nov. within the Fimbriimonadia class nov., of the phylum  
629 Armatimonadetes, *Antonie van Leeuwenhoek*, 102, 307-317, doi:10.1007/s10482-012-9739-6, 2012.
- 630 Iwai, S., Weinmaier, T., Schmidt, B. L., Albertson, D. G., Poloso, N. J., Dabbagh, K., and DeSantis, T. Z.:  
631 Piphillin: improved prediction of metagenomic content by direct inference from human microbiomes, *PloS one*,  
632 11, e0166104, doi:10.1371/journal.pone.0166104., 2016.
- 633 Janssen, P. H.: Identifying the dominant soil bacterial taxa in libraries of 16S rRNA and 16S rRNA genes, *Appl.*  
634 *Environ. Microbiol.*, 72, 1719-1728, doi:10.1128/AEM.72.3.1719-1728.2006, 2006.
- 635 Jensen, M. M., Lam, P., Revsbech, N. P., Nagel, B., Gaye, B., Jetten, M. S., and Kuypers, M. M.: Intensive  
636 nitrogen loss over the Omani Shelf due to anammox coupled with dissimilatory nitrite reduction to ammonium,  
637 *ISME J.*, 5, 1660-1670, doi:10.1038/ismej.2011.44, 2011.
- 638 Krause, S., Liebetrau, V., Löscher, C. R., Böhm, F., Gorb, S., Eisenhauer, A., and Treude, T.: Marine  
639 ammonification and carbonic anhydrase activity induce rapid calcium carbonate precipitation, *Geochim.*  
640 *Cosmochim. Acta*, 243, 116-132, doi:10.1016/j.gca.2018.09.018, 2018.
- 641 Kümmel, S., Herbst, F.-A., Bahr, A., Duarte, M., Pieper, D. H., Jehmlich, N., Seifert, J., von Bergen, M.,  
642 Bombach, P., Richnow, H. H., and Vogt, C.: Anaerobic naphthalene degradation by sulfate-reducing  
643 Desulfobacteraceae from various anoxic aquifers, *FEMS Microbiol. Ecol.*, 91, 13, doi:10.1093/femsec/fiv006,  
644 2015.
- 645 Langille, M. G., Zaneveld, J., Caporaso, J. G., McDonald, D., Knights, D., Reyes, J. A., Clemente, J. C.,  
646 Burkepille, D. E., Thurber, R. L. V., and Knight, R.: Predictive functional profiling of microbial communities  
647 using 16S rRNA marker gene sequences, *Nat. Biotechnol.*, 31, 814-821, doi:10.1038/nbt.2676, 2013.
- 648 Leloup, J., Loy, A., Knab, N. J., Borowski, C., Wagner, M., and Jørgensen, B. B.: Diversity and abundance of  
649 sulfate-reducing microorganisms in the sulfate and methane zones of a marine sediment, Black Sea, *Environ.*  
650 *Microbiol.*, 9, 131-142, doi:10.1111/j.1462-2920.2006.01122.x, 2007.
- 651 Liu, J., Sun, F., Wang, L., Ju, X., Wu, W., and Chen, Y.: Molecular characterization of a microbial consortium  
652 involved in methane oxidation coupled to denitrification under micro-aerobic conditions, *Microb. Biotechnol.*,  
653 7, 64-76, doi:10.1111/1751-7915.12097, 2014.
- 654 Löscher, C. R., Mohr, W., Bange, H. W., and Canfield, D. E.: No nitrogen fixation in the Bay of Bengal?,  
655 *Biogeosciences*, 17, 851-864, doi:10.5194/bg-17-851-2020, 2020.
- 656 Luo, H., and Moran, M. A.: How do divergent ecological strategies emerge among marine bacterioplankton  
657 lineages?, *Trends Microbiol.*, 23, 577-584, doi:10.1016/j.tim.2015.05.004, 2015.
- 658 Lv, X., Yu, J., Fu, Y., Ma, B., Qu, F., Ning, K., and Wu, H.: A meta-analysis of the bacterial and archaeal  
659 diversity observed in wetland soils, *Sci. World J.*, 2014, 1-12, doi:10.1155/2014/437684, 2014.
- 660 Madigan, M., Cox, S. S., and Stegeman, R. A.: Nitrogen fixation and nitrogenase activities in members of the  
661 family Rhodospirillaceae, *J. Bacteriol.*, 157, 73-78, doi:10.1128/JB.157.1.73-78.1984, 1984.
- 662 Maltby, J., Sommer, S., Dale, A. W., and Treude, T.: Microbial methanogenesis in the sulfate-reducing zone of  
663 surface sediments traversing the Peruvian margin, *Biogeosciences*, 13, 283-299, doi:10.5194/bg-13-283-2016,  
664 2016.
- 665 Manske, A. K., Glaeser, J., Kuypers, M. M., and Overmann, J.: Physiology and phylogeny of green sulfur  
666 bacteria forming a monospecific phototrophic assemblage at a depth of 100 meters in the Black Sea, *Appl.*  
667 *Environ. Microbiol.*, 71, 8049-8060, doi:10.1128/AEM.71.12.8049-8060.2005, 2005.
- 668 McCreary Jr, J. P., Yu, Z., Hood, R. R., Vinayachandran, P., Furue, R., Ishida, A., and Richards, K. J.: Dynamics  
669 of the Indian-Ocean oxygen minimum zones, *Prog. Oceanogr.*, 112, 15-37, doi:10.1016/j.pocean.2013.03.002,  
670 2013.



- 671 Mußmann, M., Pjevac, P., Krüger, K., and Dykema, S.: Genomic repertoire of the Woeseiaceae/JTB255,  
672 cosmopolitan and abundant core members of microbial communities in marine sediments, ISME J., 11, 1276-  
673 1281, doi:10.1038/ismej.2016.185, 2017.
- 674 Naqvi, S., Naik, H., Pratihary, A., D'Souza, W., Narvekar, P., Jayakumar, D., Devol, A., Yoshinari, T., and  
675 Saino, T.: Coastal versus open-ocean denitrification in the Arabian Sea, Biogeosciences, 3, 621-633,  
676 doi:10.5194/bg-3-621-2006, 2006.
- 677 Naqvi, S. W. A., Lam, P., Narvekar, G., Sarkar, A., Naik, H., Pratihary, A., Shenoy, D. M., Gauns, M., Kurian,  
678 S., and Damare, S.: Methane stimulates massive nitrogen loss from freshwater reservoirs in India, Nat.  
679 Commun., 9, 1265-1274, doi:10.1038/s41467-018-03607-z, 2018.
- 680 Narayan, N. R., Weinmaier, T., Laserna-Mendieta, E. J., Claesson, M. J., Shanahan, F., Dabbagh, K., Iwai, S.,  
681 and DeSantis, T. Z.: Piphillin predicts metagenomic composition and dynamics from DADA2-corrected 16S  
682 rDNA sequences, BMC genomics, 21, 1-12, doi:10.1186/s12864-020-6537-9, 2020.
- 683 Nelson, D., and Sommers, L.: Methods of soil analysis Part 2. Chemical and Microbiological Properties, in:  
684 Total Carbon, Organic Carbon, and Organic Matter, American Society of Agronomy, Soil Science Society of  
685 America, USA, 539-579, 1982.
- 686 Orsi, W. D., Coolen, M. J. L., Wuchter, C., He, L., More, K. D., Irigoien, X., Chust, G., Johnson, C.,  
687 Hemingway, J. D., Lee, M., Galy, V., and Giosan, L.: Climate oscillations reflected within the microbiome of  
688 Arabian Sea sediments, Sci. Rep., 7, 6040, doi:10.1038/s41598-017-05590-9, 2017.
- 689 Padilla, C. C., Bristow, L. A., Sarode, N., Garcia-Robledo, E., Ramírez, E. G., Benson, C. R., Bourbonnais, A.,  
690 Altabet, M. A., Girguis, P. R., and Thamdrup, B.: NC10 bacteria in marine oxygen minimum zones, ISME J.,  
691 10, 2067, doi:10.1038/ismej.2015.262, 2016.
- 692 Pattan, J., Mir, I. A., Parthiban, G., Karapurkar, S. G., Matta, V., Naidu, P., and Naqvi, S.: Coupling between  
693 suboxic condition in sediments of the western Bay of Bengal and southwest monsoon intensification: A  
694 geochemical study, Chem. Geol., 343, 55-66, doi:10.1016/j.chemgeo.2013.02.011, 2013.
- 695 Paulmier, A. D. R.-P.: Oxygen minimum zones (OMZs) in the modern ocean, Prog. Oceanogr., 80, 113-128,  
696 doi:10.1016/j.pcean.2008.08.001, 2009.
- 697 Penton, C. R., Devol, A. H., and Tiedje, J. M.: Molecular evidence for the broad distribution of anaerobic  
698 ammonium-oxidizing bacteria in freshwater and marine sediments, Appl. Environ. Microbiol., 72, 6829-6832,  
699 doi:10.1128/AEM.01254-06., 2006.
- 700 Pitcher, A., Villanueva, L., Hopmans, E. C., Schouten, S., Reichart, G.-J., and Damsté, J. S. S.: Niche  
701 segregation of ammonia-oxidizing archaea and anammox bacteria in the Arabian Sea oxygen minimum zone,  
702 ISME J., 5, 1896, doi:10.1038/ismej.2011.60, 2011.
- 703 Pramanik, A., Basak, P., Banerjee, S., Sengupta, S., Chattopadhyay, D., and Bhattacharyya, M.: Metagenomic  
704 exploration of the bacterial community structure at Paradip Port, Odisha, India, Genom. Data, 7, 94-96,  
705 doi:10.1016/j.gdata.2015.12.005, 2016.
- 706 Quast, C., Pruesse, E., Yilmaz, P., Gerken, J., Schweer, T., Yarza, P., Peplies, J., and Glöckner, F. O.: The  
707 SILVA ribosomal RNA gene database project: improved data processing and web-based tools, Nucleic Acids  
708 Res., 41, D590-D596, doi:10.1093/nar/gks1219, 2012.
- 709 Quince, C., Lanzen, A., Davenport, R. J., and Turnbaugh, P. J.: Removing noise from pyrosequenced amplicons,  
710 BMC Bioinf., 12, 38, doi:10.1186/1471-2105-12-38, 2011.
- 711 Rajpathak, S. N., Banerjee, R., Mishra, P. G., Khedkar, A. M., Patil, Y. M., Joshi, S. R., and Deobagkar, D. D.:  
712 An exploration of microbial and associated functional diversity in the OMZ and non-OMZ areas in the Bay of  
713 Bengal, J. Biosci., 43, 635-648, doi:10.1007/s12038-018-9781-2, 2018.
- 714 Ramaswamy, V., and Gaye, B.: Regional variations in the fluxes of foraminifera carbonate, coccolithophorid  
715 carbonate and biogenic opal in the northern Indian Ocean, Deep Sea Res. Part I, 53, 271-293,  
716 doi:10.1016/j.dsr.2005.11.003, 2006.
- 717 Ramos, H. C., Hoffmann, T., Marino, M., Nedjari, H., Presecan-Siedel, E., Dreesen, O., Glaser, P., and Jahn, D.:  
718 Fermentative metabolism of *Bacillus subtilis*: physiology and regulation of gene expression, J. Bacteriol., 182,  
719 3072-3080, doi:10.1128/JB.182.11.3072-3080.2000, 2000.



- 720 Robinson, R. S., Kienast, M., Luiza Albuquerque, A., Altabet, M., Contreras, S., De Pol Holz, R., Dubois, N.,  
721 Franco, R., Galbraith, E., and Hsu, T. C.: A review of nitrogen isotopic alteration in marine sediments,  
722 *Paleoceanogr.*, 27, doi:10.1029/2012PA002321, 2012.
- 723 Sarma, V., Kumar, M. D., and Saino, T.: Impact of sinking carbon flux on accumulation of deep-ocean carbon  
724 in the Northern Indian Ocean, *Biogeochemistry*, 82, 89–100, doi:10.1007/s10533-006-9055-1, 2007.
- 725 Sarma, V., Krishna, M., Viswanadham, R., Rao, G., Rao, V., Sridevi, B., Kumar, B., Prasad, V., Subbaiah, C.  
726 V., and Acharyya, T.: Intensified oxygen minimum zone on the western shelf of Bay of Bengal during summer  
727 monsoon: influence of river discharge, *J. Oceanogr.*, 69, 45–55, doi:10.1007/s10872-012-0156-2, 2013.
- 728 Schimel, J. P., and Schaeffer, S. M.: Microbial control over carbon cycling in soil, *Front. Microbiol.*, 3, 348–  
729 358, doi:10.3389/fmicb.2012.00348, 2015.
- 730 Schloss, P. D., Westcott, S. L., Ryabin, T., Hall, J. R., Hartmann, M., Hollister, E. B., Lesniewski, R. A.,  
731 Oakley, B. B., Parks, D. H., and Robinson, C. J.: Introducing mothur: open-source, platform-independent,  
732 community-supported software for describing and comparing microbial communities, *Appl. Environ.*  
733 *Microbiol.*, 75, 7537–7541, doi:10.1128/AEM.01541-09, 2009.
- 734 Schunck, H., Lavik, G., Desai, D. K., Großkopf, T., Kalvelage, T., Löscher, C. R., Paulmier, A., Contreras, S.,  
735 Siegel, H., and Holtappels, M.: Giant hydrogen sulfide plume in the oxygen minimum zone off Peru supports  
736 chemolithoautotrophy, *PloS one*, 8, e68661, doi:10.1371/journal.pone.0068661, 2013.
- 737 Shao, M.-F., Zhang, T., and Fang, H. H.-P.: Sulfur-driven autotrophic denitrification: diversity, biochemistry,  
738 and engineering applications, *Appl. Microbiol. Biotechnol.*, 88, 1027–1042, doi:10.1007/s00253-010-2847-1,  
739 2010.
- 740 Stewart, F. J., Ulloa, O., and DeLong, E. F.: Microbial metatranscriptomics in a permanent marine oxygen  
741 minimum zone, *Environ. Microbiol.*, 14, 23–40, doi:10.1111/j.1462-2920.2010.02400.x, 2012.
- 742 Suh, S.-S., Park, M., Hwang, J., Lee, S., Moh, S. H., Park, K. H., and Lee, T.-K.: Characterization of bacterial  
743 communities associated with seasonal water masses from Tongyoung in South Sea of Korea, *Ocean Sci. J.*, 49,  
744 193–200, doi:10.1007/s12601-014-0019-4, 2014.
- 745 Ulloa, O., Wright, J. J., Belmar, L., and Hallam, S. J.: Pelagic oxygen minimum zone microbial communities,  
746 in: *The Prokaryotes*, edited by: Rosenberg E., DeLong E.F., Lory S., Stackebrandt E., and F., T., Springer,  
747 Berlin, Heidelberg, 113–122, 2013.
- 748 van der Weijden, C. H., Reichart, G. J., and Visser, H. J.: Enhanced preservation of organic matter in sediments  
749 deposited within the oxygen minimum zone in the northeastern Arabian Sea, *Deep Sea Res. Part II*, 46, 807–830,  
750 doi:10.1016/S0967-0637(98)00093-4, 1999.
- 751 Varki, A., and Gagneux, P.: Biological functions of glycans, in: *Essentials of Glycobiology* [Internet]. 3rd  
752 edition, Cold Spring Harbor Laboratory Press, 2017.
- 753 Wang, Y., Sheng, H.-F., He, Y., Wu, J.-Y., Jiang, Y.-X., Tam, N. F.-Y., and Zhou, H.-W.: Comparison of the  
754 levels of bacterial diversity in freshwater, intertidal wetland, and marine sediments by using millions of illumina  
755 tags, *Appl. Environ. Microbiol.*, 78, 8264–8271, doi:10.1128/AEM.01821-12, 2012.
- 756 Ward, B., Devol, A., Rich, J., Chang, B., Bulow, S., Naik, H., Pratihary, A., and Jayakumar, A.: Denitrification  
757 as the dominant nitrogen loss process in the Arabian Sea, *Nature*, 461, 78–82, doi:10.1038/nature08276, 2009.
- 758 Wegner, C.-E., Richter-Heitmann, T., Klindworth, A., Klockow, C., Richter, M., Achstetter, T., Glöckner, F. O.,  
759 and Harder, J.: Expression of sulfatases in *Rhodopirellula baltica* and the diversity of sulfatases in the genus  
760 *Rhodopirellula*, *Mar. Genomics*, 9, 51–61, doi:10.1016/j.margen.2012.12.001, 2013.
- 761 West, N. J., Schönhuber, W. A., Fuller, N. J., Amann, R. I., Rippka, R., Post, A. F., and Scanlan, D. J.: Closely  
762 related *Prochlorococcus* genotypes show remarkably different depth distributions in two oceanic regions as  
763 revealed by in situ hybridization using 16S rRNA-targeted oligonucleotides, *Microbiology*, 147, 1731–1744,  
764 doi:10.1099/00221287-147-7-1731, 2001.
- 765 Yakimov, M. M., Giuliano, L., Gentile, G., Crisafi, E., Chernikova, T. N., Abraham, W.-R., Lünsdorf, H.,  
766 Timmis, K. N., and Golyshin, P. N.: *Oleispira antarctica* gen. nov., sp. nov., a novel hydrocarbonoclastic  
767 marine bacterium isolated from Antarctic coastal sea water, *Int. J. Syst. Evol. Microbiol.*, 53, 779–785,  
768 doi:10.1099/ijs.0.02366-0, 2003.



769 Yanagibayashi, M., Nogi, Y., Li, L., and Kato, C.: Changes in the microbial community in Japan Trench  
770 sediment from a depth of 6292 m during cultivation without decompression, FEMS Microbiol. Lett., 170, 271 -  
771 279, doi:10.1111/j.1574-6968.1999.tb13384.x, 1999.

772 Yu, Z., Wang, X., Han, G., Liu, X., and Zhang, E.: Organic and inorganic carbon and their stable isotopes in  
773 surface sediments of the Yellow River Estuary, Sci. Rep., 8, 1-10, doi:10.1038/s41598-018-29200-4, 2018.

774 Zhu, D., Tanabe, S.-H., Yang, C., Zhang, W., and Sun, J.: Bacterial community composition of South China Sea  
775 sediments through pyrosequencing-based analysis of 16S rRNA genes, PloS one, 8, e78501,  
776 doi:10.1371/journal.pone.0078501, 2013.

777

778

779